



Transthyretin Cardiac Amyloidosis Scintigraphy Using Planar D-SPECT on Dedicated Cardiac CZT Camera

Sagi Tshori, MD, PhD,^{a,b} Shay Livschitz, MD,^a Igor Volodarsky, MD,^a Sorel Goland, MD,^{a,c} Sara Shimoni, MD,^{a,c} Jacob Fabrikant, MD,^a and Jacob George, MD^{a,c}

^a Heart Center, Kaplan Medical Center, Rehovot, Israel

^b Institute of Medical Research Israel-Canada, The Hebrew University, Jerusalem, Israel

^c The Hebrew University, Jerusalem, Israel

Received Oct 1, 2020; accepted Apr 7, 2021

doi:10.1007/s12350-021-02651-5

Background. Bone scintigraphy is a main diagnostic tool in suspected ATTR patients. Almost all literature is based on conventional whole body gamma cameras, and there is very sparse data evaluating the use of dedicated cardiac CZT cameras. The aim of this study was to evaluate the utility of bone scintigraphy in suspected transthyretin cardiac amyloidosis (ATTR-CA) patients on a dedicated cardiac CZT camera.

Methods. Seventy-three patients with suspected ATTR-CA underwent planar and SPECT Tc-99m pyrophosphate scintigraphy using dedicated cardiac CZT camera between May and August 2019.

Results. Planar D-SPECT image quality was mostly good. Six patients were identified as ATTR-CA positive. Inter-observer agreement based on both Perugini score and on planar D-SPECT H/CL ratio was excellent.

Conclusions. ATTR-CA scintigraphy using dedicated cardiac CZT camera was feasible, and yielded planar D-SPECT images with excellent inter-observer agreement. (J Nucl Cardiol 2022;29:1995–2000.)

Key Words: Transthyretin • cardiac amyloidosis • scintigraphy • CZT camera • planar • SPECT • pyrophosphate

INTRODUCTION

Transthyretin cardiac amyloidosis (ATTR-CA) is a life threatening disease, and usually causes restrictive cardiomyopathy, heart failure, and conduction disorders.¹ Recently, it became common practice to base ATTR-CA diagnosis on nuclear scintigraphy, which is now further supported by multi-societal expert consensus recommendations.²

Since scintigraphy is now a cornerstone of ATTR-CA diagnosis, detailed understanding of the characteristics, techniques and pitfalls of this modality are required. However, almost all studies so far, including the breakthrough manuscript by Gilmore et al,³ were performed on conventional whole body gamma cameras. The use of cardiac dedicated CZT cameras is becoming a common practice,⁴ but very few studies using dedicated CZT camera for ATTR-CA imaging were published so far.

The authors of this article have provided a PowerPoint file, available for download at SpringerLink, which summarises the contents of the paper and is free for re-use at meetings and presentations. Search for the article DOI on SpringerLink.com.

The authors have also provided an audio summary of the article, which is available to download as ESM, or to listen to via the JNC/ASNCPodcast.

Supplementary Information The online version contains supplementary material available at <https://doi.org/10.1007/s12350-021-02651-5>.

Reprint requests: Sagi Tshori, MD, PhD, Heart Center, Kaplan Medical Center, Pasternak St., 1, Rehovot 7661041, Israel; sagit@ekmd.huji.ac.il

1071-3581/\$34.00

Copyright © 2021 American Society of Nuclear Cardiology.

In the current study we assessed the feasibility and the utility of dedicated CZT ATTR-CA imaging, assessing inter-observer agreement for both visual scoring and for D-planar H/CL ratio.

METHODS

Study Population

Between May and August 2019, 73 consecutive patients sent for scintigraphy in Kaplan Medical Center due to suspected ATTR-CA were enrolled. The protocol was approved by the Kaplan Medical Center Institutional Review Board and subjects provided informed consent. All enrolled patients tested negative for the presence of free serum light chains. Light chain amyloidosis was excluded by serum free light chain assay and serum/urine immunofixation.

Imaging Protocol

Patients were administered 740 MBq (20 mCi) of Tc-99 m Pyrophosphate (PYP). SPECT images, and an additional planar acquisition, were obtained using a D-SPECT Cardio dedicated CZT camera (Spectrum Dynamics). The D-SPECT camera incorporates 9 swiveling CZT detectors, each able to swivel independently, with all detectors performing orbital motions to close the gaps between detectors. While in 3D SPECT imaging each detector will swivel and collect 60 angular views per orbital position, for true planar imaging all detectors will be oriented to the same direction and collect 1 angular view per orbital position. The acquired scan then provides multiple small 64×16 pixels which can be combined into a larger 64×128 pixels true planar image which is equivalent to that of a conventional SPECT planar image.

Prior to D-SPECT true planar acquisition and as a surrogate to the P-scope used on conventional camera, an initial 10 seconds pre-scan is performed while detector head is placed ~ 2.5 cm below patient sternum. The pre-scan will generate a series of planar images at ± 15 degrees around the anterior view to enable the user to select the best anterior view for the true planar acquisition and ensure optimal patient positioning.

Five minute planar scans and 10 minutes SPECT scans were obtained. Median time to scintigraphy was 81 minutes (IQR 67-103 minutes).

Imaging Interpretation

All scans were independently interpreted by two experienced readers (S.T and S.L). Visual interpretation was performed using the Perugini scoring system⁵: 0-absent cardiac uptake and normal bone uptake; 1-mild cardiac uptake, lower than bone uptake; 2-moderate cardiac uptake and reduced bone uptake; 3-strong cardiac uptake with mild/absent bone uptake. Planar heart to contralateral ratio (H/CL) was obtained by placing an adjustable ROI according to cardiac uptake. When there was no uptake the ROI was set according to anatomical location, as would be done with a p-scope. An ROI of the same size was then positioned on the opposite side according to anatomical location, using the same method as for a conventional camera. The ratio was then calculated using the manufacturers' Matlab H/CL calculation routine with default parameters.

Statistical Analysis

Statistical analysis was performed using SPSS version 25.0 (IBM). Inter-observer agreement for ordinal data (visual scoring) was evaluated using Cohen's kappa (κ) test with linear weighting. Inter-observer agreement on H/CL ratios was assessed using type C two-way mixed effects average score model for

Table 1. Patient characteristics (n = 73)

Age (years)	70 (61.5-76.5)
Male	43 (59)
BMI (kg/m ²)	28.1 (23.9-32.1)
NYHA class (n = 65)	
I	20 (31)
II	23 (35)
III	22 (34)
Co-morbidities	
Hypertension (n = 64)	43 (67)
Hyperlipidemia (n = 61)	45 (74)
Obesity (n = 65)	18 (28)
Smoking (n = 63)	14 (22)
Ischemia (n = 63)	6 (10)
Echocardiography	
LVEF (%)	45 (36-55)
IVSD (mm)	12 (10-14)
LVPW (mm)	10 (9-12)
LAA (cm ²)	23 (19-27)

Values are represented as median (interquartile range) or n (%).

LVEF, left ventricular ejection fraction; LAA, left atrial area; IVSD, interventricular septal thickness at diastole; LVPW, left ventricular posterior wall

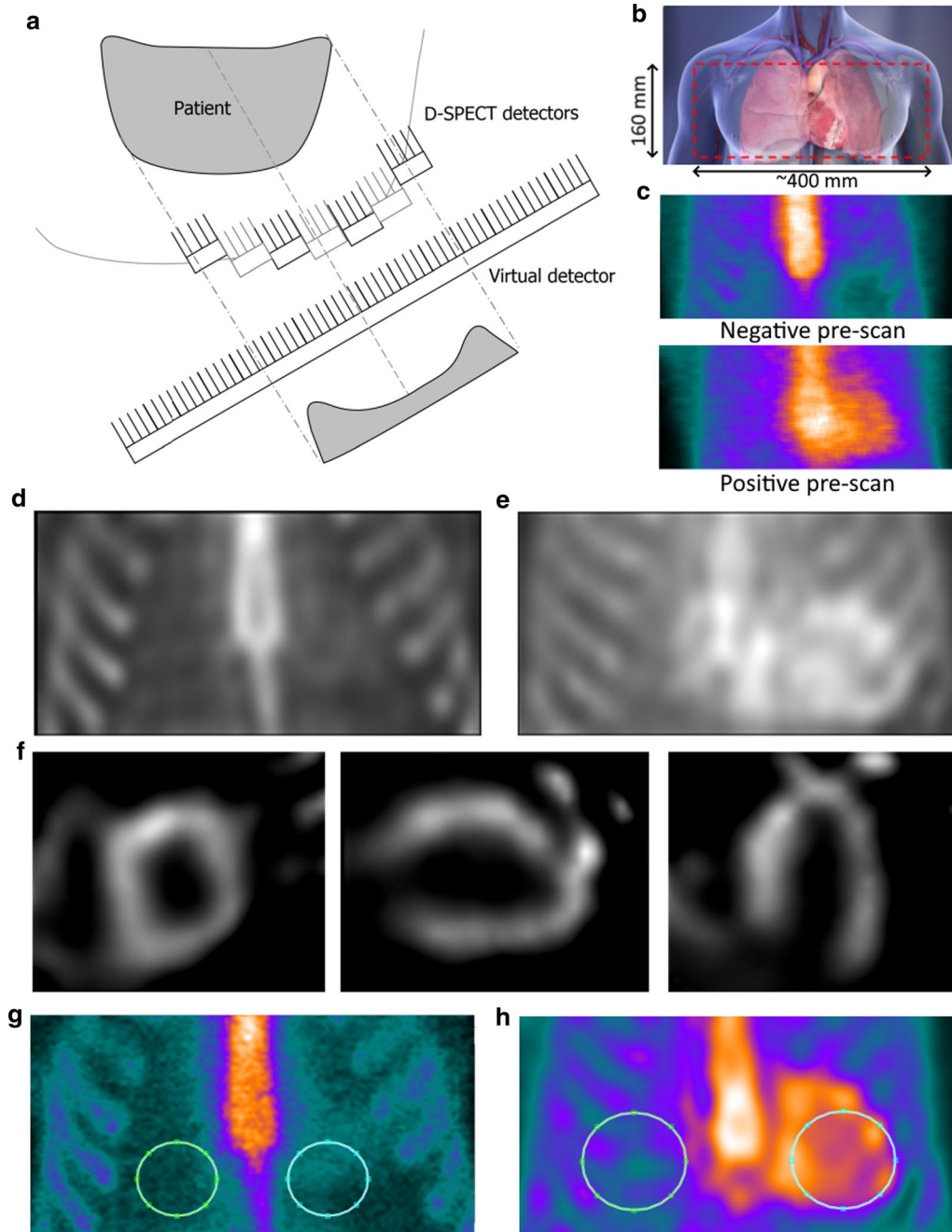


Figure 1. Planar D-SPECT and SPECT ATTR-CA scintigraphy in dedicated cardiac CZT camera. (A) Schematic representation of the virtual planar D-SPECT detector. (B) Schematic representation of camera vertical and horizontal FOV placed on the chest during ATTR-CA scintigraphy. (C) 10 second pre-scan of negative and positive patients are presented. The pre-scans are used to adjust the placement of the detector head and the angle for optimal anterior view. (D, E) Planar D-SPECT image of a negative (D) and positive (E) ATTR-CA scan. (F) Short axis and long axes SPECT images of the same positive patient. (G, H) ROI placement for H/CL ratio calculation in negative (G) and positive (H) scans.

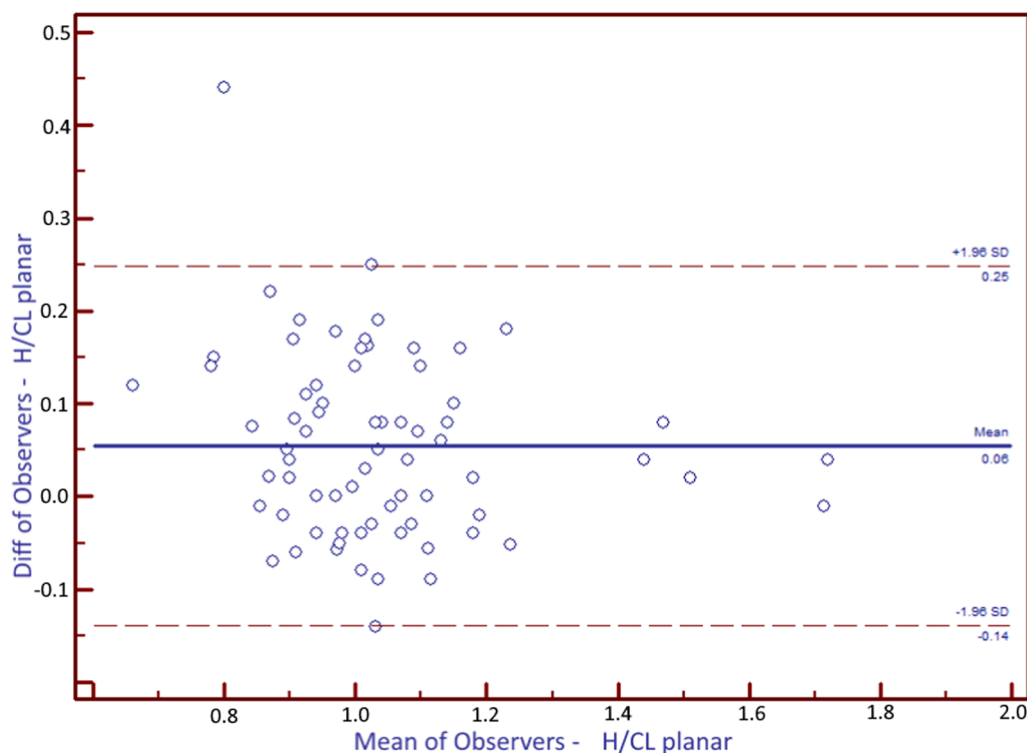


Figure 2. Bland-Altman plots of differences in D-planar H/CL ratio between observers. Lines represent mean \pm 1.96 SD values.

Table 2. ICC for visual score and for D-planar H/CL ratios

Method	ICC (95% CI)	P value
Negative/positive	1.000 (1.000-1.000)	<.001
Perugini VS	0.941 (0.906-0.963)	<.001
D-planar H/CL	0.930 (0.888-0.956)	<.001

Type C two-way mixed effects model Interclass correlation coefficients (ICC). Negative (Perugini 0-1) and positive (Perugini 2-3). Visual score (VS) across all four Perugini categories. Mean and 95% confidence intervals are shown

interclass correlation coefficient (ICC (C,2)). Bland-Altman graphs were plotted for H/CL ratio inter-observer agreement. Two tailed p values were calculated. $P < .05$ was considered statistically significant in all tests.

RESULTS

Study Population

Overall 73 patients were included in the study. Patient characteristics are summarized in Table 1. Patients were predominantly males (43/73, 59%), distributed between NYHA class I to III (Table 1). All patients underwent Tc-99 m PYP scintigraphy using a dedicated D-SPECT camera.

Planar D-SPECT Imaging

Patients were pre-scanned for 10 second for optimal positioning (Figure 1A, B). Using low statistic planar images, the lower part of the detector head was placed \sim 2.5 cm below the patient's sternum, and the best view for the planar acquisition was assessed. For most patients a target angle of 0 degrees, as selected from the pre-scan cine images, was considered to provide the optimal planar view; however, for some patients a slight adjustment of the angle, by usually no more than \pm 2 degrees, was required for optimization of the planar view. Image quality was considered as good for almost all planar and SPECT images (Figure 1C-E).

Visual Scoring and D-Planar H/CL Ratio

Visual analysis of planar scans was performed using Perugini score.⁵ Six patients were identified as ATTR positive. Blood pool and overlying bone uptake were ruled out using the SPECT images.

All six patients were identified as positive (Perugini score 2-3) by both observers in both early and late planar scans. Inter-observer agreement on individual categories of the Perugini score was very good with Cohen's κ score 0.815 (95% CI 0.695-0.936).

H/CL ratios were calculated on D-planar images using a Matlab procedure developed by the manufacturer. Inter-observer differences were assessed using Bland-Altman plots (Figure 2). Inter-observer agreement was very good, and the difference values were largely clustered around the zero line.

Interclass correlation coefficients (ICC) were calculated for negative (Perugini 0-1) vs positive (Perugini 2-3), for visual score across all Perugini scores, and for D-planar H/CL ratios (Table 2). Inter-observer agreement was excellent for visual scoring. Excellent agreement was also observed for D-planar H/CL ratio (ICC 0.930, 95% CI 0.888-0.956, $P < .001$).

DISCUSSION

Diagnosis of ATTR-CA currently relies on bone scintigraphy.⁶ There is currently very little published experience with dedicated cardiac CZT cameras. Our study describes the acquisition and analysis of D-planar images. Our study indicates that D-planar ATTR-CA scintigraphy can be performed on dedicated cardiac CZT camera (Spectrum Dynamics) with excellent inter-observer agreement. Inter-observer reproducibility of H/CL ratio was studied using a conventional SPECT/CT camera.⁷ Bland-Altman plots revealed up to $\pm 20\%$ difference using the common ± 1.96 SD limits. In the current study similar to slightly lower differences were observed.

Currently, no large scale comparison of D-SPECT and A-SPECT H/CL ratios was yet published. However, heart to mediastinum ratio using I-123 MIBG and Tc-99m tetrofosmin phantoms yielded high correlation between planar D-SPECT and planar A-SPECT.⁸ High linear correlation was found between heart to contralateral ratio and Perugini grade.⁹ Furthermore, high correlation between planar D-SPECT and A-SPECT H/CL ratio was found in a single center study of 50 patients.¹⁰

Study limitations

Recent studies have identified ATTR-CA in 13% of the patients with HF with preserved ejection fraction,¹¹ and 5% of patients with presumed hypertrophic cardiomyopathy.¹² Our policy was to broaden the indications for ATTR-CA scintigraphy, thus expecting a lower positive rate. This policy is in accordance with recent position and consensus statements.¹³ Indeed, despite being sufficiently powered, we had only six (8.2%) positive patients in our study cohort, while many studies are designed with 50% or more positive patients.^{3,14}

CONCLUSION

ATTR-CA scintigraphy using dedicated CZT cardiac camera yields high quality planar images. Inter-observer agreement on visual scoring was excellent, and inter-observer agreement on D-planar H/CL ratio was very good.

NEW KNOWLEDGE GAINED

Planar D-SPECT ATTR-CA scintigraphy can be performed on dedicated cardiac CZT. Excellent inter-observer agreement was observed for both planar visual score based on Perugini criteria and D-planar H/CL ratio.

Acknowledgements

We would like to thank Dalia Shiti, Refael Baavour and Justine McQuillan for their help in the production of images and in the technical details of the D-SPECT planar image acquisition.

Disclosures

All authors have nothing to disclose.

References

1. Rubin J, Maurer MS. Cardiac amyloidosis: Overlooked, underappreciated, and treatable. *Ann Rev Med.* 2020;71:203–19.
2. Dorbala S, Ando Y, Bokhari S, Dispenzieri A, Falk RH, Ferrari VA, et al. ASNC/AHA/ASE/EANM/HFSA/ISA/SCMR/SNMMI expert consensus recommendations for multimodality imaging in cardiac amyloidosis: Part 1 of 2-evidence base and standardized methods of imaging. *J Cardiac Fail.* 2019;25:e1–39.
3. Gillmore JD, Maurer MS, Falk RH, Merlini G, Damy T, Dispenzieri A, et al. Nonbiopsy diagnosis of cardiac transthyretin amyloidosis. *Circulation.* 2016;133:2404–12.
4. Hyafil F, Gimelli A, Slart RHJA, Georgoulas P, Rischpler C, Lubberink M, et al. EANM procedural guidelines for myocardial

- perfusion scintigraphy using cardiac-centered gamma cameras. *Eur J Hybrid Imaging*. 2019;3:11.
5. Perugini E, Guidalotti PL, Salvi F, Cooke RM, Pettinato C, Riva L, et al. Noninvasive etiologic diagnosis of cardiac amyloidosis using ^{99m}Tc -3,3-diphosphono-1,2-propanodicarboxylic acid scintigraphy. *Journal of the American College of Cardiology*. 2005;46:1076–84.
 6. George J, Rappaport M, Shimoni S, Goland S, Voldarsky I, Fabricant Y, et al. A novel monoclonal antibody targeting aggregated transthyretin facilitates its removal and functional recovery in an experimental model. *Eur Heart J*. 2020;41:1260–70.
 7. Singh V, Cuddy S, Kijewski MF, Park MA, Taylor A, Taqueti VR, et al. Inter-observer reproducibility and intra-observer repeatability in (^{99m}Tc -pyrophosphate scan interpretation for diagnosis of transthyretin cardiac amyloidosis. *J Nucl Cardiol Cardiology*. 2020. <https://doi.org/10.1007/s12350-020-02353-4>.
 8. Bellevre D, Manrique A, Legallois D, Bross S, Baavour R, Roth N, et al. First determination of the heart-to-mediastinum ratio using cardiac dual isotope (^{123}I -MIBG/ ^{99m}Tc -tetrofosmin) CZT imaging in patients with heart failure: The ADRECARD study. *Eur J Nucl Med Mol Imaging*. 2015;42:1912–9.
 9. Manrique A, Dudoignon D, Brun S, N'Ganoa C, Cassol E, Legallois D, et al. Quantification of myocardial (^{99m}Tc -labeled bisphosphonate uptake with cadmium zinc telluride camera in patients with transthyretin-related cardiac amyloidosis. *EJNMMI Res*. 2019;9:117.
 10. Mahmood U, Feldkamp M, Rosamond T. ATTR Cardiac Amyloidosis: A direct comparison between conventional gamma camera heart/lung ratio quantification and D-SPECT methodology in 50 consecutive patients. *J Nucl Med*. 2020;61:1616.
 11. Gonzalez-Lopez E, Gallego-Delgado M, Guzzo-Merello G, de Haro-Del Moral FJ, Cobo-Marcos M, Robles C, et al. Wild-type transthyretin amyloidosis as a cause of heart failure with preserved ejection fraction. *Eur Heart J*. 2015;36:2585–94.
 12. Damy T, Costes B, Hagege AA, Donal E, Eicher JC, Slama M, et al. Prevalence and clinical phenotype of hereditary transthyretin amyloid cardiomyopathy in patients with increased left ventricular wall thickness. *Eur Heart J*. 2016;37:1826–34.
 13. Dorbala S, Ando Y, Bokhari S, Dispenzieri A, Falk RH, Ferrari VA, et al. ASNC/AHA/ASE/EANM/HFSA/ISA/SCMR/SNMMI expert consensus recommendations for multimodality imaging in cardiac amyloidosis: Part 2 of 2-Diagnostic criteria and appropriate utilization. *J Nucl Cardiol*. 2020;27:659–73.
 14. Flaherty KR, Morgenstern R, Pozniakoff T, DeLuca A, Castano A, Maurer MS, et al. (^{99m}Tc)Technetium pyrophosphate scintigraphy with cadmium zinc telluride cameras is a highly sensitive and specific imaging modality to diagnose transthyretin cardiac amyloidosis. *J Nucl Cardiol*. 2019. <https://doi.org/10.1007/s12350-019-01831-8>.

Publisher's Note Springer Nature remains neutral with regard to jurisdictional claims in published maps and institutional affiliations.